

Baryon deceleration by strong chromofields in ultrarelativistic nuclear collisions

Igor N. Mishustin^{1,2} and Konstantin A. Lyakhov³

¹*Frankfurt Institute for Advanced Studies,*

J.W. Goethe University, D-60438 Frankfurt am Main, Germany

²*The Kurchatov Institute, Russian Research Center, 123182 Moscow, Russia*

³*Frankfurt International Graduate School for Science,*

J.W. Goethe University, D-60438 Frankfurt am Main, Germany

Abstract

It is assumed that strong chromofields are generated at early stages of ultrarelativistic heavy-ion collisions which give rise to a collective deceleration of net baryons from colliding nuclei. We have solved classical equations of motion for baryonic slabs under the action of a time-dependent longitudinal chromoelectric field. It is demonstrated that the slab final rapidities are rather sensitive to the strength and decay time of the chromofield as well as to the back reaction of the produced partonic plasma. The net-baryon rapidity loss $\langle \delta y \rangle = 2.0$, found for most central Au-Au collisions at RHIC, can be explained by the action of chromofields with the initial energy density of about 50 GeV/fm³. Predictions for the baryon stopping at the LHC are made.

PACS numbers: 25.75.-q, 12.38.Mh, 24.10.Jv, 24.85.+p

arXiv:hep-ph/0612069 v1 6 Dec 2006

It is expected that strong chromofields can develop at early stages of ultrarelativistic heavy-ion collisions. There exist different suggestions concerning the space-time structure of these fields, ranging from string-like configurations as in the color Flux Tube Model (FTM) [1] to stochastic configurations associated with the Color Glass Condensate (CGC) [2]. This picture is most conveniently presented in the c. m. frame where two Lorentz contracted nuclei look as thin sheets. After their intersection these sheets acquire stochastic color charges as a result of multiple soft gluon exchange. Then strong chromofields are generated in the space between the receding sheets. At later times these fields decay into quarks and gluons which after equilibration form a quark-gluon plasma. This process has been studied by several authors under different assumptions about the field decay mechanism (see e. g. Refs. [3, 4, 5]).

Most previous calculations assume that after interaction the nuclear debris follow the light-cone trajectories, thus disregarding their energy losses to produce the chromofield. This assumption can be possibly justified only at asymptotically high energies. Furthermore, this assumption becomes irrelevant when studying the baryon stopping. Obviously, the energy of produced fields and particles is taken entirely from the kinetic energy of the colliding nuclei.

As measured by the BRAHMS collaboration [6], in central Au+Au collisions at highest RHIC energy $\sqrt{s_{NN}} = 200$ GeV per NN -pair the baryon energy losses are very significant, about 70% of the initial energy. The net-baryon rapidity distributions are substantially shifted toward the center of mass from the initial rapidities $\pm y_0$.

The problem of baryon stopping at RHIC has been addressed recently by several authors. In particular, net-baryon rapidity distributions were calculated within the microscopic string-based models like UrQMD [7] and QGSM [8]. Although these models implement energy and momentum conservation, and thus predict a certain baryon stopping, they are formulated in momentum space and do not give a space-time picture of this process. Also, they are dealing with hadronic secondaries and therefore preclude the quark-gluon plasma formation. Recently, the calculations have been also done within a parton cascade model [9]. The distribution of valence quarks at central rapidities was also studied in ref. [10] within a QCD motivated approach which however can not be extended to the fragmentation regions.

In ref.[11] a simple space-time model was proposed where the baryon stopping was directly linked to the formation of strong chromofields. There nuclear trajectories were calculated

under assumption that the field is neutralized at a sharp proper time 1 fm/c (see also refs. [12, 13]). In this paper we further develop this model and apply it for a more realistic decay pattern of the chromofield. Our main goal is to calculate the net-baryon rapidity distribution and compare it with the BRAHMS data.

Following ref. [14] we decompose the collision of two ultrarelativistic nuclei into a set of pairwise collisions of elementary slabs. At given impact parameter \vec{b} the positions of the target and projectile slabs in the transverse plane are determined by vectors \vec{s} and $\vec{b} - \vec{s}$, respectively. The transverse cross section area of individual slabs is assumed to coincide with the nucleon-nucleon inelastic cross section σ_{NN} . The energy and momentum of the projectile ($a = p$) and target ($a = t$) slabs are parameterized as $E_a = M_a \cosh Y_a$ and $P_a = M_a \sinh Y_a$, where $M_a = m_\perp N_a$ is the average transverse mass and N_a is the average baryon number of slab a . The average baryon transverse mass m_\perp differs from the free nucleon mass m_N due to internal excitation of slabs acquired at the interpenetration stage. It is parameterized in terms of the mean transverse momentum as $m_\perp = \sqrt{m_N^2 + \langle p_\perp \rangle^2}$. The calculations below are made in light-cone coordinates, proper time $\tau = \sqrt{t^2 - z^2}$ and space-time rapidity $\eta = \frac{1}{2} \ln \left(\frac{t+z}{t-z} \right)$.

In the Glauber model (see e.g. refs. [15, 16]) the average number of participating nucleons from nucleus a in a slab of transverse area σ_{NN} located at a radius-vector \vec{s} is given by the expression

$$N_a(\vec{b}, \vec{s}) = \sigma_{NN} A_a T_a(\vec{b} - \vec{s}) \left(1 - [1 - \sigma_{NN} T_{\bar{a}}(\vec{s})]^{A_{\bar{a}}} \right), \quad (1)$$

where $\bar{a} = t$ for $a = p$ and vice versa, A_a is the mass number of nucleus a . The normalized functions T_a ($a = p, t$) describe the transverse profiles of the baryon number distribution in colliding nuclei. They are obtained by the integration of the corresponding baryon densities along the beam direction, $A_a T_a = \int \rho_a(\vec{r}) dz$. The average number of nucleon-nucleon collisions in an inelastic interaction of two slabs at a radius-vector \vec{s} is expressed as

$$N_{\text{coll}}(\vec{b}, \vec{s}) = \sigma_{NN}^2 A_p T_p(\vec{b} - \vec{s}) A_t T_t(\vec{s}). \quad (2)$$

We assume that the initial energy density stored in the chromofield after collision of two baryonic slabs can be parameterized as

$$\epsilon_f(\tau_0; \vec{b}, \vec{s}) = \epsilon_0 \left(\frac{s}{s_0} \right)^\alpha \left[N_{\text{coll}}(\vec{b}, \vec{s}) \right]^\beta, \quad (3)$$

where ϵ_0 is the fitting parameter, second factor describes the collision energy dependence with $\alpha \approx 0.3$, as motivated by small x behavior of the gluon structure function [17]. The last factor describes effects of the collision geometry, where exponent β is related to the spatial distribution of the chromofield. For non-overlapping strings $\beta \approx 1.0$, but in the case of string clustering β is expected to be closer to 0.5 [18]. In this paper we consider only the case $\beta = 1$.

The equations of motion for a baryonic slab under the action of the longitudinal uniform chromofield are obtained by applying the energy-momentum conservation laws across the slab. It is assumed that the space between the receding slabs is occupied by the chromofield and a partonic plasma, produced by the partial field decay. They exert a certain force on the slab from inside. But from the other side the slab has nothing but the physical vacuum. This results in a net force acting on the slab. The final system of differential equations governing the slab rapidities $Y_a(\tau)$ has the following form (detailed calculations see in ref. [19])

$$\frac{d\tilde{P}_a}{d\tau} = \mp B(\tau) - \frac{\tilde{P}_a}{\tau}, \quad (4)$$

$$\frac{dM_a^2}{d\tau} = \mp 2A(\tau)\tilde{P}_a, \quad (5)$$

$$\frac{d\eta_a}{d\tau} = \mp \frac{\tilde{P}_a}{\tau\tilde{E}_a}, \quad (6)$$

where $\tilde{P}_a = M_a \sinh(Y_a - \eta_a)$, $\tilde{E}_a = \sqrt{M_a^2 + \tilde{P}_a^2}$, $B(\tau) = \sigma_{NN}(\epsilon_{vac} + \epsilon_f - p)$ and $A(\tau) = \sigma_{NN}(\epsilon_p + p)$. The plus and minus signs in the r. h. s. of these equations correspond to the projectile ($a = p$) and target ($a = t$) slabs, respectively. We adopt the initial conditions for the slab trajectories $\eta_a(\tau_0) = Y_a(\tau_0) = \pm y_0$ at $\tau_0 = 0.01$ fm, where $\pm y_0$ are the initial c.m. rapidities of colliding nuclei. In expressions above ϵ_p and $p = c_s^2 \epsilon_p$ are, respectively, the energy density and pressure of the partonic plasma, and c_s is the sound velocity. The vacuum energy density ϵ_{vac} (bag constant) is introduced to account for the fact that the chromofield and partonic plasma can exist only in the perturbative vacuum. In numerical calculations ϵ_{vac} is fixed to the value 0.4 GeV/fm³. It is assumed that the chromofield energy density $\epsilon_f(\tau)$ and the plasma energy density $\epsilon_p(\tau)$ are functions of the proper time τ only, defined in the interval $\eta_t(\tau) \leq \eta \leq \eta_p(\tau)$. The plasma energy density, $\epsilon_p(\tau)$ is found from

the hydrodynamical equation with a source term due to the field decay:

$$\frac{d\epsilon_p}{d\tau} + (1 + c_s^2) \frac{\epsilon_p}{\tau} = -\frac{d\epsilon_f}{d\tau} . \quad (7)$$

We integrate the Eqs. (4)-(6) until the time when the total pressure in the region between the slabs vanishes, i.e. $B(\tau) = 0$. After this time the slabs move with constant velocity. Obviously, the solution of equation (4) is

$$\tilde{P}_a = \tilde{P}_a(\tau_0) \frac{\tau_0}{\tau} \mp \frac{1}{\tau} \int_{\tau_0}^{\tau} B(\tau) \tau d\tau , \quad (8)$$

and the slab rapidity $Y_a(\tau)$ can be easily found from the definition $\tilde{P}_a = M_a \sinh(Y_a - \eta_a)$. Then, the slab trajectory, $z_a(\tau)$, is obtained from the relation $z_a = \tau \sinh \eta_a$.

Below we present results for Au+Au and d+Au collisions at maximum RHIC energy $\sqrt{s_{NN}}=200$ GeV per NN pair ($y_0 = 5.4$). The nucleon-nucleon inelastic cross section was taken to be $\sigma_{NN} = 42$ mb [16]. The baryon mean transverse momentum $\langle p_{\perp} \rangle$, which determines the internal energy of baryonic slabs, was fixed at the value 1.0 GeV/c, in accordance with BRAHMS data [6] for midrapidity region.

We have considered several functional forms for the time dependence of the chromofield, resulting in different plasma production rates and baryon deceleration patterns. Here we present results for the power law, $\epsilon_f(\tau) = \epsilon_f(\tau_0) \left[1 + \frac{\tau - \tau_0}{\tau_d}\right]^{-4}$ characterized by the decay time $\tau_d = 0.6$ fm/c, as expected for the Schwinger-like decay mechanism [3]). This function is shown in Fig. 1 together with the time dependence of the plasma energy density as predicted by the hydrodynamical equation (7). According to our picture, the Quark-Gluon Plasma(QGP) is produced by the continuous transformation of the field energy into the quark-antiquark and gluon pairs. Because of the delayed production, the plasma energy density is always smaller than the initial energy density of the chromofield. In accordance with previous calculations [3], we find that it reaches only about 22% of the latter for the Schwinger-like decay law.

Figs. 2 shows how the time evolution of the slab rapidities $Y_{p,t}(\tau)$ depends on the initial energy density of the chromofield, as well as on the baryon numbers of colliding slabs. The ideal equation of state ($c_s^2=1/3$) was used for the quark-gluon plasma. We present results for several values of the parameter ϵ_0 (see eq. (3)) between 0.5 and 2.0 GeV/fm³. Upper panels show results for the collision of two equal slabs with baryon numbers $N_p = N_t=5.8$,

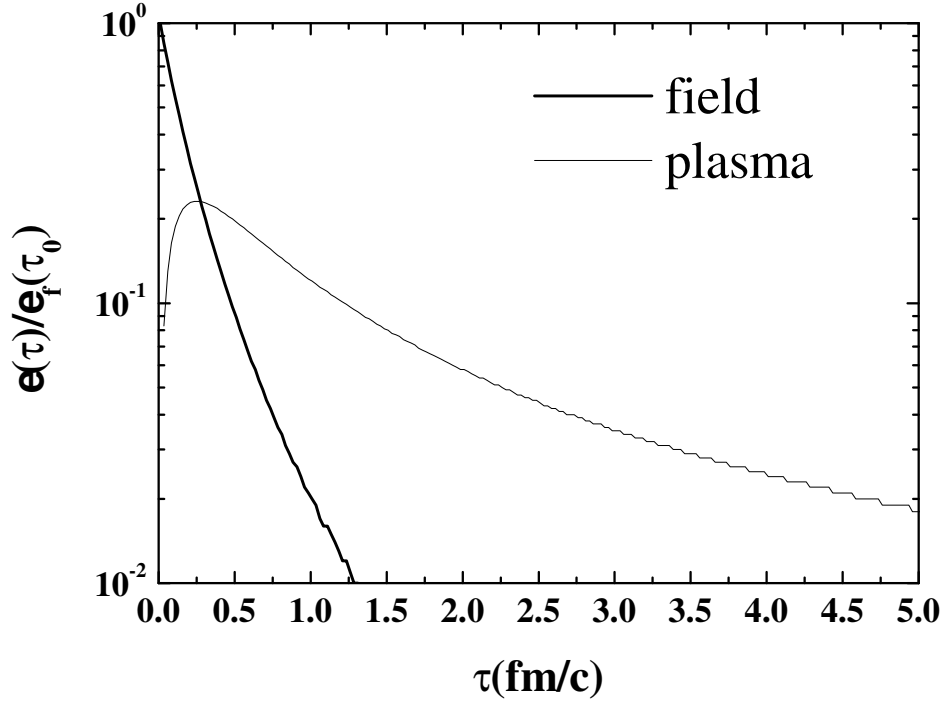


FIG. 1: Evolution of the chromofield energy density (thick solid line) and QGP energy density (thin solid line) in units of the initial chromofield energy density $\epsilon_f(\tau_0)$. Results are shown for the Schwinger-like (power-law) decay mechanism with $\tau_d = 0.6$ fm/c.

representing an average pair of slabs in a central Au+Au collision. The initial energy densities of the chromofield, $\epsilon_f(\tau_0)$, range in this case from 16.8 (lower curves) to 67.3 (upper curves) GeV/fm³. According to the BRAHMS data [6] the mean baryon rapidity loss for the most central Au-Au collisions is $\langle \delta y \rangle \approx 2.0$. From the figures one can see that slab rapidities $Y_{p,t}(\tau)$ drop rapidly at very early stages of the deceleration process, when the field is still strong. At later times, not only the decreasing chromofield (see Fig. 1) but also the plasma counter-pressure (left panels) cause an early termination of the deceleration process. As the result, the asymptotic slab rapidities have a low sensitivity to the initial chromofield energy density. Nevertheless, the observed rapidity loss can be achieved with the initial field energy density $\epsilon_f(\tau_0) = 50 \div 70$ GeV/fm³. On the other hand, it is likely that the plasma pressure in the vicinity of the slabs is not as strong as in the central region. Then the deceleration process will be less affected by the plasma, and resulting slabs' rapidities will be smaller. This is illustrated in the right panels showing calculations of the slab rapidities ignoring the

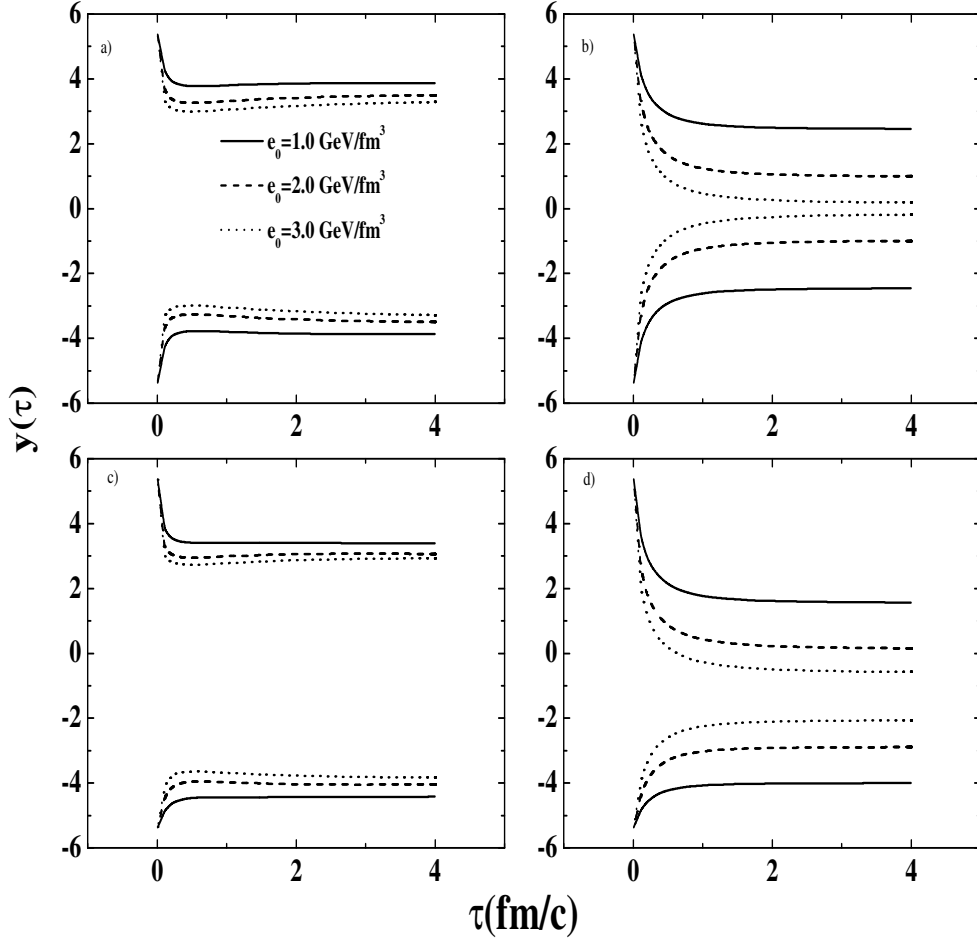


FIG. 2: Projectile (upper curves) and target (lower curves) slab rapidities as functions of proper time calculated for the power-law chromofield decay with $\tau_d=0.6$ fm/c. Different pairs of curves correspond to different values of the parameter ϵ_0 (indicated in the figure). Results are shown for two cases: a,b) equal slabs with $N_p = N_t = 5.8$ representing a central Au+Au collision, and c,d) two different slabs with $N_p=2$, $N_t=8.8$ representing a central d+Au collision. Left and right panels show the calculations with and without the back reaction of the produced plasma, respectively.

plasma pressure. In this case the required rapidity loss can be achieved with a much weaker chromofield, $\epsilon_f(\tau_0) \approx 30 \div 40$ GeV/fm³. It is clear that the realistic situation will be in between of these two extremes.

Low panels show results for an asymmetric collision of $N_p=2$ and $N_t=8.8$ slabs, which

can be interpreted as a deuteron colliding with a center of a gold nucleus. The parameter ϵ_0 is the same as before but now it corresponds to $\epsilon_f(\tau_0)$ between 8.9 and 35.5 GeV/fm³. One can see that the rapidity shifts are now different for the light and heavy slabs. Moreover, the rapidity lost by the smaller slab is significantly larger as compared with the bigger one. This is of course a direct consequence of the fact that equal forces generate a larger deceleration for a smaller body. It is interesting to note that the mean rapidity loss of a deuteron-like nucleus in a d+Au collision is predicted to be about two times larger than the mean rapidity loss of the gold nuclei in a central Au+Au collision.

In Fig. 3 we present the net-baryon rapidity distributions calculated for the central Au+Au collisions at maximum RHIC energy $\sqrt{s_{NN}}=200$ GeV per NN -pair. The calculations were done by applying Gaussian weights for different color charges generated on the slabs [2]. Since the energy density of the chromofield is proportional to the square of the areal charge density, like in a capacitor, these weights are exponential in terms of the field energy density, i.e. $P(\epsilon_f) \propto \exp\left[-\frac{\epsilon_f}{\langle\epsilon_f\rangle}\right]$, where $\langle\epsilon_f\rangle \equiv \epsilon_f(\tau_0)$ is the mean energy density of the field as parameterized in eq. (3). The introduction of the fluctuating field leads to a very interesting effect: although the zero field has a maximum probability, quite large values of the field, comparable with $\langle\epsilon_f\rangle$, are possible with a certain probability too. The larger fields lead to larger decelerations of the slabs. As a result, the dN_B/dy distribution has a long tail towards central rapidities. This is exactly what is observed by the BRAHNS collaboration [6].

The results shown in Fig. 3 were obtained without back reaction of the partonic plasma on the baryon deceleration. As one can see, in this case we can get a perfect fit of the data by choosing $\epsilon_0 \approx 1$ GeV/fm³, which, according to eq. (3), corresponds to the actual field energy density of about 35 GeV/fm³. Inclusion of the back reaction of plasma would require increasing of the initial chromofield energy density or/and the field decay time.

On the basis of our model we can make predictions for the net-baryon dynamics for the future LHC experiments. We use eq. (3) to extrapolate the initial field energy density from the RHIC ($\sqrt{s_0}=200$ GeV) to the LHC ($\sqrt{s}=5500$ GeV) energy domain. Then we get the mean net-baryon rapidity loss between 2.7 and 5.5 units for the calculation with and without the back reaction of partonic plasma, respectively.

In conclusion, the collective deceleration of valence (net) baryons was studied assuming that strong longitudinal chromofields are formed at early stages of an ultrarelativistic heavy-

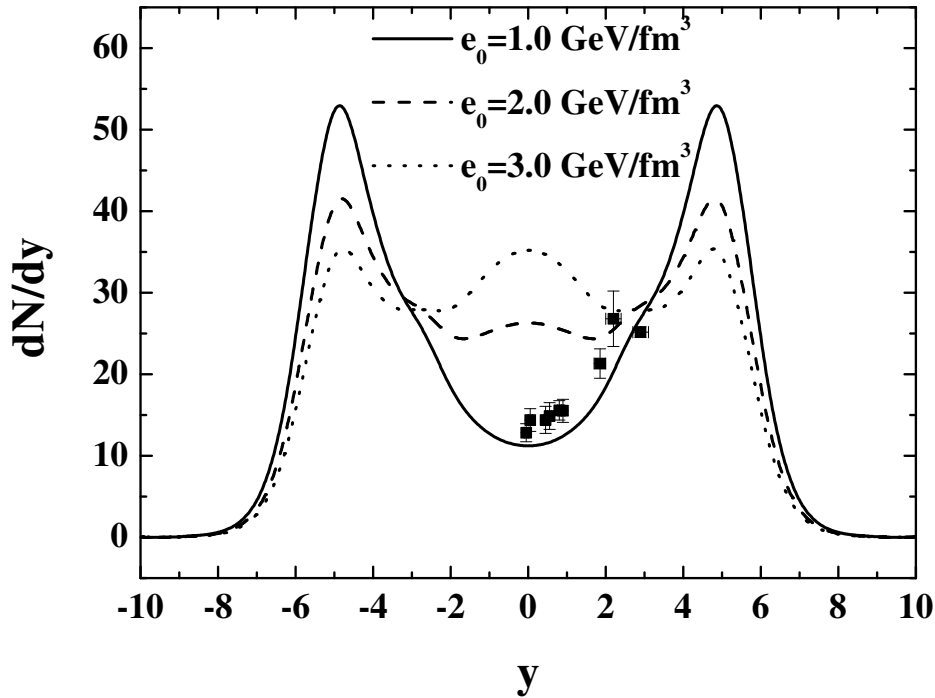


FIG. 3: Net-baryon rapidity distribution in central Au+Au collisions ($N_{\text{part}}=380$) at $\sqrt{s_{NN}} = 200$ GeV per NN -pair calculated for 3 different values of the parameter ϵ_0 (indicated in the figure). Back reaction of the partonic plasma is not included in the calculation of the slab rapidities. Dots are experimental data of BRAHMS collaboration [6].

ion collision. We have solved classical equations of motion for baryonic slabs under the action of a time-dependent chromoelectric field. A simple hydrodynamical consideration shows that the energy density of produced plasma, due to the delayed production, is always significantly lower than the initial energy density of the chromofield. It has been demonstrated that the net-baryon rapidity loss $\langle \delta y \rangle \approx 2$ can be achieved with the initial energy density of the chromofield in the range of 40 to 70 GeV/fm³. The calculated net baryon rapidity distributions for central Au+Au collisions at RHIC energies are in good agreement with BRAHMS data. The mean net-baryon rapidity loss for central Pb+Pb collisions at LHC energies is predicted between 2.7 and 5.5 units.

More detailed results, including the rapidity densities of net baryons and partonic plasma, calculated for different field decay patterns and centrality classes, will be presented in the forthcoming publication [19].

The authors thank C. Greiner, M. Gyulassy, L. McLerran, L.M. Satarov and H. Stöcker for useful discussions. This work was supported in part by the DFG grant 436RUS 113/711/0-2 (Germany), and grants RFFR-05-02-04013 and NS-8756.2006.2. (Russia).

- [1] A. Casher, H. Neuberger, and S. Nussinov, Phys. Rev. D **20** (1979); N. K. Glendenning and T. Matsui, Nucl. Phys. **B245**, 449 (1984); K. Kajantie and T. Matsui, Phys. Lett. **164B**, 373 (1985); M. Gyulassy and A. Iwazaki, Phys. Lett. **165B**, 157 (1985).
- [2] L. McLerran, and R. Venugopalan, Phys. Rev. D **49**, 2233 (1994); D **49**, 3352 (1994); E. Jancu and L. McLerran, Phys. Lett. **B510**, 145 (2000); L. McLerran, Nucl. Phys. **A699**, 73 (2002).
- [3] G. Gatoff, A. K. Kerman, and T. Matsui, Phys. Rev. D **36**, 114 (1987); K.J. Eskola and M. Gyulassy, Phys. Rev. C **47** 2329 (1993).
- [4] A. Kovner, L. McLerran, and H. Weigert, Phys. Rev. D **52**, 3809 (1995); *ibid* D **52**, 6231 (1995).
- [5] F. Gelis, K. Kajantie and T. Lappi, Phys. Rev. C **71**, 024904 (2005).
- [6] I.G. Bearden and BRAHMS Collaboration, Phys. Rev. Lett. (2004).
- [7] S.A. Bass et al., Prog. Part. Nucl. Phys. **41**, 225 (1998).
- [8] N.S. Amelin, N. Armesto, C. Pajares, D. Souza, Eur. Phys. J. C **22**, 149 (2001).
- [9] Steffen A. Bass, Berndt Müller and Dinesh K. Srivastava, Phys. Rev. Lett. **91**, 052302 (2005).
- [10] K. Itakura, Yu. Kovchegov, L. McLerran, D. Teaney, Nucl. Phys. **A730**, 160-190 (2004).
- [11] I.N. Mishustin, J.I. Kapusta, Phys. Rev. Lett. **88**, 112501 (2002).
- [12] V.K. Magas, L.P. Csernai, D. Strottman, Nucl. Phys. **A712**, 167 (2002).
- [13] Reiner J. Fries, Josef I. Kapusta and Yang Li, hep-ph/0511101.
- [14] Yu.B. Ivanov, I.N. Mishustin, L.M. Satarov, Nucl. Phys. **A443**, 713 (1985).
- [15] C.Y.Wong, *Introduction to High-Energy Heavy-Ion Collisions* (World Scientific, Singapore 1994)
- [16] D. Kharzeev, M. Nardi Phys.Lett.**B57**, 121-128(2001)
- [17] Dmitri Kharzeev, Eugene Levin, Phys. Lett. **B523** 79 (2001).
- [18] M.A. Braun, , F. del Moral, and C. Pajares, Phys. Rev. **C65**, 024907 (2002).
- [19] I.N. Mishustin and K.A. Lyakhov, paper in preparation.